



TRABALHO FINAL

MESTRADO INTEGRADO EM MEDICINA

Clínica Universitária de Imagiologia

Microvascular invasion in hepatocellular carcinoma: anatomic-radiological correlation

Tiago Filipe Serrano Constantino

Orientado por:

Professora Doutora Sofia Reimão

Co-Orientado por:

Dra. Maria Inês Leite

Maio 2023

Resumo

O Carcinoma Hepatocelular (CHC) é a terceira principal causa de morte relacionada com o cancro no mundo. A invasão microvascular (IVM) é um fator prognóstico essencial nos doentes com CHC e representa uma ferramenta valiosa para a previsão de recorrência e a seleção adequada de tratamento.

Neste estudo, retrospectivo analisou-se a importância do desempenho diagnóstico da Ressonância Magnética (RM) na avaliação pré-operatória e previsão de IVM, comparando os resultados RM e histológicos em doentes com CHC utilizando diversos *softwares* especializados.

A amostra foi constituída por incluídos 22 doentes que foram tratados cirurgicamente para CHC no Hospital de Santa Maria, entre abril de 2017 e março de 2022, realizando previamente uma RM abdominal, com contraste extracelular ou hépato-específico.

Em relação aos dados demográficos, as variáveis estudadas não demonstraram distribuição normal. Quanto à fiabilidade interobservador, todas as lesões medidas na fase portal, hépato-específica, bem como todos o ROIs medidos neste estudo, nas sequências T1 em fase e fora de fase, e na sequência T2 mostraram uma consistência excepcional (coeficiente $>0,950$). Na análise da relevância das características de RM preditores de IVM, as medições efetuadas na fase portal, hépato-específica, *Washout* e a hipervascularidade das lesões demonstraram terem relevância na predição de IVM ($p < 0,05$). Foi observada na maioria das variáveis uma fiabilidade intraobservador excelente (coeficiente $>0,900$). Não foi possível demonstrar o papel preditor das variáveis significativas na IVM ($p = 0,080$).

Alguns resultados observados neste estudo estão de acordo com a literatura, como as medições das lesões na fase portal, hépato-específico e na análise do *Washout* e da hipervascularidade das lesões de CHC. Estes achados sugerem que as características de RM apresentam potencial menos invasivo para predizer IVM no doentes com diagnóstico de CHC.

Palavras-chave: Carcinoma Hepatocelular, Invasão Microvascular, Ressonância Magnética.

Abstract

Hepatocellular Carcinoma (HCC) is the third leading cause of cancer-related death worldwide. Microvascular invasion (MVI) is a key prognostic factor in patients with HCC and represents a valuable tool for predicting recurrence and appropriate treatment selection.

This retrospective study analyzed the importance of Magnetic Resonance Imaging (MRI) diagnostic performance in preoperative evaluation and prediction of MVI by comparing MRI and histological findings in HCC patients using several specialized software.

The sample consisted of included 22 patients who were surgically treated for HCC at Santa Maria Hospital in Lisbon between April 2017 and March 2022, previously performing an abdominal MRI, with extracellular or hepatocyte-specific contrast.

Regarding demographic data, the studied variables did not show normal distribution. Regarding interobserver reliability, all lesions measured in the portal, hepatobiliary phase, as well as all ROIs measured in this study, on T1 in-phase and out-of-phase sequences, and T2 sequence showed exceptional consistency (coefficient $>0,950$). In the analysis of the relevance of MRI features predictors of MVI, measurements performed in portal phase, hepatospecific, Washout and hypervascularity of lesions were shown to have relevance in predicting MVI ($p < 0,05$). Excellent intraobserver reliability (coefficient $>0,900$) was observed for most variables. The predictive role of significant variables of MVI could not be demonstrated ($p = 0,080$).

Some results observed in this study are in agreement with the literature, such as the measurements of lesions in the portal and hepatobiliary phase and the analysis of Washout and hypervascularity of HCC lesions. These findings suggest that MRI features have potential as less invasive method to predict MVI in patients with HCC.

Keywords: Hepatocellular Carcinoma, Microvascular Invasion, Magnetic Resonance Imaging.

O trabalho final é da exclusiva responsabilidade do seu autor, não cabendo responsabilidade à FMUL pelos conteúdos nele apresentados.

Index

Resumo.....	3
Abstract	3
Index of figures	6
Introduction	7
1. Theoretical concepts/Background	10
1.1. Hepatic Tumors	10
1.1.1. Hepatocellular carcinoma	11
1.2. Histology of Hepatocellular Cancer	13
1.2.1. Premalignant lesions on HCC: DNs Low-grade and High-grade	14
1.2.2. Early and Advance HCC: Histologic, molecular pathology and the difference on imaging features	15
1.2.3. Microvascular invasion	17
1.3. The role of Magnetic Resonance Imaging in Hepatocellular cancer	18
1.3.1. MRI LI-RADS Classification	19
2. Materials and Methods	22
2.1. Patients and Methods.....	22
2.2. Image analysis and MRI Protocol	22
2.3. Histopathologic Analysis	24
2.4. Statistical data	24
3. Results and Discussion.....	25
3.1. Group Characterisation	25
3.2. Analysis of MRI features as predictors of MVI.....	26
3.2.1. Reliability of MRI Features analysis interobserver	27
3.2.2. Analysis of predictors of MVI in Observer 1, 2 and 3	28
3.2.3. Reliability of MRI Features analysis intraobserver	31
3.2.4. Microvascularity invasion predicted by MRI features	33
4. Limitations and Futures Perspectives	34
5. Conclusions	36
6. Acknowledgments	38
7. References.....	39

Index of figures

Figure 1 – Worldwide estimated age-standardized incidence rates of Liver cancer in 2020.....	9
Figure 2 – Worldwide estimated age-standardized mortality by Liver cancer in 2020...	10
Figure 3 – Tumours of hepatocyte origin	12
Figure 4 – CT/MRI Diagnostic algorithm.....	18
Figure 5 – The eight categories of LI-RADS and each approach	19
Figure 6 – Bar graphic displaying the percentage of subjects by sex.....	24
Figure 7 – Axial plane T1 fat saturation with HBP contrast showing hypointensity lesion.	25

Introduction

Hepatocellular carcinoma (HCC) is a worldwide health challenge that is ranked as the seventh most common cancer and the third leading cause of cancer-related death. In contrast, HCC is ranked in Portugal as the tenth most common and deadly cancer (Sung et al., 2021).

Cirrhosis is the most critical clinical risk factor for HCC and nearly 80% of cases of HCCs arise in a background of underlying cirrhotic liver (Clark et al., 2015; Hartke et al., 2017). Several studies have shown that hepatocarcinogenesis implies the stepwise progression of a tumor from a high-grade dysplastic nodule in a cirrhotic liver to advanced HCC (Fattovich et al., 2004; Hartke et al., 2017; Li, Chen, et al., 2019). With the advancement and development of magnetic resonance imaging (MRI), the rate of early detection is increasing, especially for small HCC ($\leq 3\text{cm}$). Although small HCCs usually have better outcomes than larger HCCs, a subset of small HCCs has been identified as more aggressive, with poorer prognosis (Fattovich et al., 2004; He et al., 2020).

Despite the advances in diagnosis and treatment, the prognosis of HCC is still poor, and the overall survival is still low due to the high rate of recurrence after curative treatment (Cabrera & Nelson, 2010a; Krinsky & Shanbhogue, 2021; L. Wang et al., 2022; Zech et al., 2020). According to the guidelines of the European Association for the Study of the Liver and the American Association for the Study of Liver Diseases, the recommended treatment for early-stage HCC includes hepatectomy, radiofrequency ablation (RFA), and liver transplantation based on liver function (Cabrera & Nelson, 2010; Dimitroulis et al., 2017; Hartke et al., 2017). Although hepatectomy is recommended as the mainstream curative treatment for HCC with well-preserved liver function, HCC recurrence at 5 years occurs in 70% of cases, indicating either multicentric relapse or intrahepatic metastases (Dimitroulis et al., 2017; Hartke et al., 2017). Moreover, the survival outcomes were improved with the application of the treatment strategies available, such as hepatectomy, liver transplantation, transarterial chemoembolization (TACE), transarterial radioembolization, radiofrequency ablation, nontargeted chemotherapy, and hepatic arterial infusion (S. J. Ahn et al., 2019; Lee et al., 2017).

Several studies have been performed which show that the prognostic factors of HCC involve chronic active hepatitis, cirrhosis, and hepatitis C virus (HCV) positivity (Fattovich et al., 2004; McGlynn et al., 2021; Sagnelli et al., 2020). Additionally, tumor size, histological differentiation, macro or microvascular invasion, and microsatellite nodules are also important prognostic indicators (S. J. Ahn et al., 2019; Sagnelli et al., 2020).

Macrovascular (defined as tumor tissue found in the portal vein, bile duct, or hepatic vein) and microvascular invasion (MVI - determined by a histopathological examination) are well-known major prognostic factors of HCC (H.-D. Zhang et al., 2023; L. Zhang et al., 2020). Macrovascular invasion can be easily assessed before surgery by imaging modalities, such as computed tomography (CT) and MRI. However, a correct preoperative MVI prediction, either by CT or MR, has not been achieved yet, which means it is still highly dependent on histopathological evaluation (Min et al., 2020; L. Wang et al., 2022). Nevertheless, it is important to identify preoperative imaging biomarkers for MVI evaluation, since it is a valuable tool for early recurrence prediction (namely within the first 2 years after curative treatment (An et al., 2015; Kim et al., 2022) and for appropriate treatment selection.

Several studies have demonstrated the potential of some preoperative imaging biomarkers for predicting MVI of HCC, such as tumor size, arterial rim enhancement, or peritumoral enhancement, tumor margin, tumor hypointensity on hepatobiliary phase (HBP), radiological capsule on gadoteric acid-enhanced MRI, higher tumor-to-liver signal intensity ratio and lower apparent diffusion coefficient (ADC) value on diffusion-weighted (DWI) with ADC map (Sim et al., 2022; Tang, 2020; Wang et al., 2022).

Although these studies have shown the potential of predicting MVI, there is still some controversy and debate over which best reflects MVI of HCC and may best predict potential early recurrence of HCC after hepatectomy. Ahn et al. proposed that arterial peritumoral enhancement was associated with a high probability of MVI (J. C. Ahn et al., 2021; L. Wang et al., 2022). Kim et al. also reported that only peritumoral hypointensity on HBP was significant in predicting MVI, whereas Arizumi et al. demonstrated that only a non-smooth margin was an independent predictor of MVI (L. Wang et al., 2022; Xu et al., 2014). Some studies have also shown the importance of tumor size, HCC larger than

5 cm in maximum diameter revealed a greater chance of presenting with MVI (Sim et al., 2022; Tang, 2020).

The principal motivation for carrying out this research is to demonstrate the importance of the role of MRI in predicting the microvascular invasion (MVI) on HCC thus allowing patient risk stratification and optimal treatment selection.

The thesis is organized as follows:

1. Theoretical concepts /background
2. Materials and methods
3. Results and discussion
4. Limitations of this study
5. Conclusions.

1. Theoretical concepts/Background

1.1. Hepatic Tumors

In 2020, 905,677 people were diagnosed with liver cancer, and 830,180 died of this condition. According to GLOBOCAN 2020, there is wide geographic variability in incidence (figure 1) and mortality (figure 2) with most of the cases occurring in developing countries. It is more common in men than in women (Llovet et al., 2021).

The burden of liver cancer is rising worldwide, which means that every country needs to encourage risk factors prevention (namely viral hepatitis prevention in the case of HCC tumors), an early diagnosis, and provide an optimal therapy selection in order to reduce morbidity and mortality (Llovet et al., 2021).

The liver can be a major locale of the development of abundant vascular, metabolic, infectious, and neoplastic processes which can be primary or secondary. For example, primary hepatic cancers such as HCC and cholangiocarcinoma are common in the presence of chronic diffuse liver diseases, whereas metastases result from other cancers, especially from gastrointestinal tumors, and are more common in the normal liver (Cabrera & Nelson, 2010).

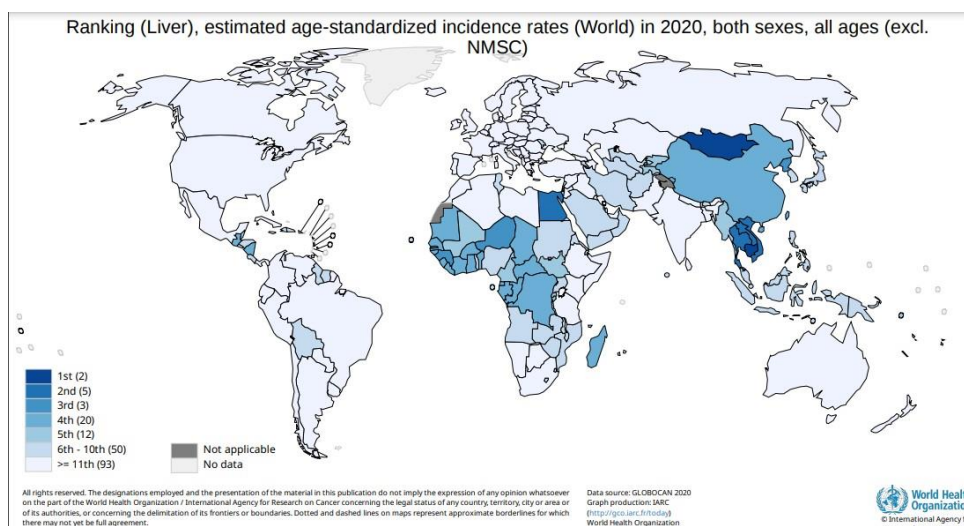


Figure 1 - Worldwide estimated age-standardized incidence rates of Liver cancer in 2020 in both genders (Llovet et al., 2021).

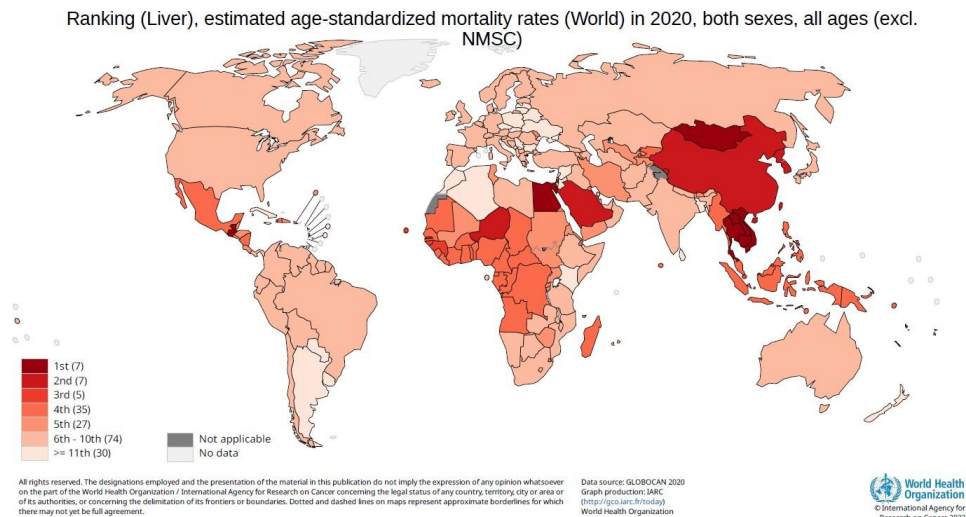


Figure 2 - Worldwide estimated age-standardized mortality by Liver cancer in 2020 in both genders (Llovet et al., 2021).

1.1.1. Hepatocellular carcinoma

Primary liver cancer is mainly divided into two major histological types: HCC, which comprises around 75% of all cancer cases, and intrahepatic cholangiocarcinoma (ICC), which represents 12-15% of cases (McGlynn et al., 2021; Sagnelli et al., 2020). The cancer incidence rates vary from 5.1 per 100,000 person-years in Europe to 17.7 per 100,000 person-years in eastern Asia (Desai et al., 2019; Sagnelli et al., 2020; Sung et al., 2021). This wide-ranging geographical and environmental variation primarily indicates local differences in the prevalence of risk factors, particularly for HCC (Desai et al., 2019; McGlynn et al., 2021; Sagnelli et al., 2020). The presence of liver disease or cirrhosis is one of the most relevant risk factors for HCC incidence, and at least 60% of HCC cases worldwide are caused by viral hepatitis. Chronic hepatitis B virus (HBV), which is frequently acquired at birth or early childhood, particularly in developing countries, remains the leading cause of HCC (Desai et al., 2019; Clark et al., 2015). On the contrary, in developed countries, hepatitis C virus (HCV) infections, acquired later in life, are far more common, but the prevalence of non-alcoholic fatty liver disease (NAFLD) associated to HCC is increasing (Darren et al., 2022; Desai et al., 2019;). According to literature, approximately a third of the world population has NAFLD which can progress to cirrhosis and HCC. Nowadays, in USA and parts of Europe, NAFLD is the quickest emerging cause of hepatocellular carcinoma, and is estimated to increase exponentially in parallel with the worldwide spread of obesity (Darren et al., 2022) Moreover,

metabolic causes (eg, hemochromatosis, Wilson disease, α 1-antitrypsin deficiency syndrome) and dietary aflatoxin exposure represent other risk factors (Clark et al., 2015; Darren et al., 2022).

Worldwide, the greatest risk factor for HCC is chronic HBV infection counting for more than 50% of cases and which is the major risk factor in Eastern Asia (Sagnelli et al., 2020). Several studies (Desai et al., 2019; Kulik & El-Serag, 2019; Sagnelli et al., 2020) reported that the incidence of HCC rises with viral load and duration of infection.

In developed countries, HCV infection and alcohol are still the most common risk factor for these tumors, with rates dependent on the local prevalence of infections (Fitzmaurice et al., 2017; Kulik & El-Serag, 2019). The high incidence of intravenous drug use, needle sharing, and unsafe sexual practice during the 1960s and 1970s increased the incidence of HCV, and with that, the HCC incidence increased as well during the 1980s and 1990s (Fitzmaurice et al., 2017; Llovet et al., 2021).

According to the last report of ECDC for 2019, 29 EU/EEA Member States reported 37,773 cases of HCV infection, representing 8.9 per 100,000 population (McGlynn et al., 2021). Whereas in EUA, from 2010 to 2019, the number of expected annual acute HCV infections augmented by 387% (McGlynn et al., 2021). This significant increase is attributed mostly to the opioid epidemic issue and is associated with intravenous drug use, especially among the young. The CDC estimated a total of 57,500 new acute cases of HCV in 2019 (McGlynn et al., 2021; Sagnelli et al., 2020).

Relative to alcohol, its consumption is common in the Americas and Western Europe, and it is increasing in Asia (Renne et al., 2021). The risk for HCC in decompensated alcohol-induced cirrhosis approaches 1% per year. It's also relevant to mention that the risk does not decrease with abstinence, and HCC may occur in a noncirrhotic liver (Kraglund et al., 2023). Several studies (Fattovich et al., 2004; Kraglund et al., 2023; Renne et al., 2021) showed the synergism of alcohol use in chronic hepatitis C which can make the risk twice as high as compared with the risk of hepatitis C alone (Fattovich et al., 2004; Renne et al., 2021). Studies in the United States and Italy suggest that for some populations alcohol is the most common cause of HCC (accounting for 32%–45% of HCC) (Fattovich et al., 2004; Renne et al., 2021). Alcohol use is increasing in many countries,

indicating that alcohol consumption will remain a common cause of HCC worldwide (Petrick et al., 2016).

NAFLD refers to a spectrum of liver disorders ranging from steatosis to its more aggressive manifestation non-alcoholic steatohepatitis (NASH). Regarding NAFLD as a risk factor, hepatocellular carcinoma is associated with a higher percentage (33%) of patients without cirrhosis (Darren et al., 2022). Darren et al., referred in his systematic reviewed that 20% of patients with steatosis or NAFLD progress to NASH-cirrhosis, from which approximately 3% undergo further development to HCC (Darren et al., 2022). Some studies imply lower surveillance outcomes than HCC due to other causes (Darren et al., 2022). In fact, newer studies are suggesting the development of surveillance strategies for patients with NAFLD without cirrhosis who are at high risk of developing HCC (Darren et al., 2022).

Considering the number of deaths from liver cancer which doubled in the past 30 years, the European Association for the Study of the Liver (EASL) recommend screening for hepatocellular cancer with an ultrasound examination every six months to reduce mortality. However, the European Commission's Group of Chief Scientific Advisors (GCSA) believe that there is not enough evidence for such a recommendation (EASL., 2022).

1.2. Histology of Hepatocellular Cancer

In the past 40 years, success in the diagnosis of early-stage HCC has improved due to the advances in diagnostic imaging modalities and the establishment of follow-up programs for high-risk populations (Kojiro, 2005; Schlageter et al., 2014). Liver nodules range from benign to dysplastic or even to malignant HCC (Cabrera & Nelson, 2010). Some small well-differentiated HCCs, are not correctly differentiated from dysplastic nodules (DN) which are considered premalignant lesions (Schlageter et al., 2014) and frequently develop into HCC, as documented frequently in follow-up imaging (Schlageter et al., 2014). The classical histopathology of HCC and unusual morphological features in HCC are presented in figure 3 (Kojiro, 2005).

Benign
Liver cell adenoma
Premalignant lesion
Low-grade dysplastic nodule (adenomatous hyperplasia)
Borderline malignancy
High-grade dysplastic nodule (atypical adenomatous hyperplasia)
Malignant
Hepatocellular carcinoma:
Grade
Well differentiated
Moderately differentiated
Poorly differentiated
Undifferentiated
Variants
Scirrhous
Sarcomatous
Fibrolamellar
Combined hepatocellular and cholangiocellular carcinoma (primary liver cancer of intermediate type, hepatic stem cell carcinoma)

Figure 3 - Tumours of hepatocyte origin (Llovet et al., 2021).

1.2.1. Premalignant lesions on HCC: DNs Low-grade and High-grade

The histopathological spectrum of premalignant lesions includes regenerative nodules and DN. Regenerative nodules involve hepatocytes and nearly always contain some intact portal tracts with a normal finding. DNs are defined as large hepatic nodules that are different from the surrounding liver parenchyma and may be subclassified as low or high grade (Kojiro et al., 2005). When DN is present, the low-grade nodules usually grow and mature to high-grade, however some of them can revert. Lower grade DNs have nodular appearance with no atypia and slight rise in cell density (Kojiro et al., 2005). Higher DNs are more likely to show nodular pattern with architectural and/or cytologic atypia, however the atypia is not enough for a diagnosis of HCC (Kojiro et al., 2005). Additionally, small HCC (less than 2 cm) can be divided into 2 subtypes: early HCC and progressed HCC (Kojiro et al., 2005). The first one is well differentiated and has a nearly nodular aspect. The second has a precisely nodular pattern and is mainly moderately differentiated, frequently revealing MVI (Kojiro et al., 2005).

1.2.2. Early and Advance HCC: Histologic, molecular pathology and the difference on imaging features

In terms of macroscopic findings, HCCs up to around 2 cm are divided into two types: a distinctly nodular type and an indistinctly nodular type (Fattovich et al., 2004; Marrero et al., 2018). It is important to recognize the difference between these two types because they diverge in their morphology and biological behaviour. The distinctly nodular type is seen as a clear nodule with a fibrous capsule and/or fibrous septa in about 50% of the cases (J. C. Ahn et al., 2021). On the other hand, the indistinctly nodular lesions usually show only a roughly nodular growth with indistinguishable margins (Kojiro et al., 2005). Concerning the histologic findings, 80% of distinctly nodular small HCCs are classified as moderately differentiated and 20% are well differentiated (Kojiro et al., 2005). For differentiating early HCC from premalignant lesions, the stromal invasion has been considered as the most useful morphological evidence (L. Wang et al., 2022). Well-differentiated early-stage HCCs are described by the following main histologic features: frequent acinar and/or pseudoglandular pattern, increased nuclear/cytoplasm ratio, and an irregular thin trabecular pattern; increased eosinophilic or basophilic staining intensity; and frequent fatty change and/or clear alteration of cancer cells (Tang, 2020).

Regarding macroscopically the advanced HCC, the architecture is modified by several factors such as the tumor diameter, the previous existence of liver cirrhosis, thrombus in the portal veins, hemorrhage, intrahepatic metastasis, and necrosis (Kojiro et al., 2005). Frequently, advanced HCC shows a nodular appearance with fibrous capsules and septa (Hartke et al., 2017; Schlageter et al., 2014). The prevalence of these last two findings is closely associated with tumor size. As mentioned before, capsule and septum formations are rare in small HCCs (<2 cm) due to not growing expansively (Schlageter et al., 2014). However, in lesions that have a diameter between 1,5–2,0 cm the tumor cells begin to grow wider, and in about 70% of these tumors both capsule and septum are formed (Schlageter et al., 2014). Regarding the lesions bigger than 2,0 cm, almost every lesion has capsule and septum.

HCC is a typical tumor that exclusively receives arterial blood supply through arterial tumor vessels and is classified as a hypervascular tumor at contrast imaging such as angiography, enhanced CT, and enhanced MRI (Silva et al., 2009). Nevertheless, most

small HCCs of indistinct nodular type are not observed as hypervascular lesions. They are not hypervascular as evidenced by insufficient development of unpaired arteries, partial capillarization of the sinusoid, and the absence of a fibrous capsule (Silva et al., 2009).

The latest developments in molecular pathology have expanded the knowledge of the genetic background of HCCs. Molecular variations in tumors reflect the differences in biologic behaviour of tumors in the same clinical stage, and could have effects on adapting therapies and foreseeing clinical outcomes (Krinsky and Shanbhogue, 2021). Nault J. and Zucman-Rossi J., mentioned in their studies that several molecular classifications have been proposed for HCC with varied histologic features based on genomic profiling and next generation sequencing (Krinsky and Shanbhogue, 2021). They referred to two distinct subgroups of HCC (proliferative and nonproliferative) as well, based on genomic variations and/or oncogenic pathways, histopathologic features and clinical outcomes (Krinsky and Shanbhogue, 2021).

The proliferative subtype has highly heterogeneous characteristics considered by its genomic pathways related to cellular proliferation and survival (Krinsky and Shanbhogue, 2021). This subtype is aggressive with poor to moderate cellular differentiation, macrotrabecular architecture, high alfa fetoprotein levels, high MVI invasion, high tumor recurrence and poor clinical outcomes (Krinsky and Shanbhogue, 2021).

On contrary, the nonproliferative subtype, retains hepatocyte-like features, resembling normal hepatic physiology with an immune response or activation of Wnt signaling pathway (Krinsky and Shanbhogue, 2021). This subtype is less aggressive with moderately to well differentiated tumor at histologic examination, lower alfa fetoprotein levels, lower tumor recurrences, and better clinical outcomes (Krinsky and Shanbhogue, 2021).

Regarding the imaging findings, Kang and Kim et al demonstrated the difference between those two subtypes based on imaging features, such as rim arterial phase enhancement (APHE), hypointense signal, and peritumoral hyperintensity on hepatobiliary phase of gadoxetate- enhanced MRI (Krinsky., and Shanbhogue, 2021). The proliferative HCCs showed more rim APHE, larger arterial phase hypo-enhancement, and

are correlated with higher rate of metastasis and poorer overall survival (Krinsky., and Shanbhogue, 2021).

1.2.3. Microvascular invasion

Vascular invasion in HCC can be either macrovascular or microvascular. The first one can be determined by gross tissue assessment or diagnostic imaging, however the latter, the MVI, is determined by a histopathological examination (Kojiro, 2005; W. Wang et al., 2021). There are many definitions and standards of MVI, however, the most common tends to be a web of malignant cells lining the vascular endothelial cells of hepatic and portal venous systems (Kojiro, 2005; W. Wang et al., 2021). Several studies have demonstrated that the incidence of MVI oscillates between 15 and 57.1% in HCC patients (Kojiro, 2005; W. Wang et al., 2021). When MVI is present, it implies that HCC cells have invaded blood vessels and may have the potential of metastasizing (Renne et al., 2021; W. Wang et al., 2021). To metastasize, according to literature, nets of hepatocellular carcinoma cells can be involved and surrounded by endothelial cells to survive in the blood and escape the immune system (Kojiro, 2005; Renne et al., 2021).

MVI is a relevant pathological predictor of the risk of the postoperative recurrence of HCC and guides for surgical planning and postoperative treatment strategies (Lei et al., 2016; W. Wang et al., 2021).

In order to accurately predict MVI in HCC, several aspects need to be assessed and analyzed. For a valuable clinical prediction scheme, multiple factors need to be analyzed, such as tumor classification, tumor diameter, degree of tumor differentiation, pathological grade, HBV DNA load, steroids hormones, tumor capsule integrity, alfa-fetoprotein level and imaging features (W. Wang et al., 2021). Lei, Z. et al demonstrated in approximately 1000 samples of HBV-related HCC that the presence of multiple and large tumors, an incomplete capsule, high level of α -fetoprotein level, HBV DNA load greater than 104 IU/ml, platelet count less than $100 \times 10^3/\mu\text{l}$, and the presence of dynamic pattern on contrast-enhanced MRI, were significantly related with MVI (Lei et al., 2016).

1.3. The role of Magnetic Resonance Imaging in Hepatocellular cancer

The several major advancements in field gradient technology and multichannel surface coils permit MRI to play an increasingly greater role in the precision, detection and characterization of hepatic lesions (Mulé et al., 2020; L. Zhang et al., 2020). CT has long been the traditional method of image for clinical hepatic diseases because of its relatively lower cost, shorter acquisition times, and broader accessibility. Nevertheless, MRI shows similar lesion patterns as CT, but with superior contrast resolution and without the use of ionizing radiation (Lee et al., 2017).

Additionally, new pulse sequences, such as diffusion-weighted (DWI) and steady-state free precession (SSFP), along with hepatocyte-specific contrast agents (eg, gadobenate dimeglumine [Gd-BOPTA {benzyloxypropionictetraacetate}]), help an earlier diagnosis of the lesion (Alvin et al., 2009).

As is well-known, there is a spectrum of lesions, from regenerative nodules, DN and HCC. So, a precise and definitive differentiation among these nodules can be interesting because of the substantial overlap in imaging and histologic features. Nonetheless, patients with untreated disease, normally have a median survival time of 6–9 months, whereas if early liver transplantation can be provided, patients have an opportunity for a cure (Hartke et al., 2017). Consequently, imagiology, preferably with MRI, plays a critical role in early diagnosis and consequent management and prognosis. Usually, T1-weighted imaging shows isointense HCC lesions, if the lesions have less than 1.5 cm, whereas larger lesions may be hyperintense secondary to lipid, glycogen, or cooper (Li, Yan, et al., 2019; Tang, 2020). Most HCC lesions at T2-weighted imaging are hyper or isointense (Tang, 2020); however, hypointense lesions can be observed particularly in well-differentiated tumors (Tang, 2020).

In patients with cirrhosis, a hypervascular lesion with an increased T2 signal similar to that of the spleen is suspicious for HCC (Lee et al., 2017; Alvin et al., 2009). At DWI, these lesions may have an inconstant appearance that depends on their histologic features; if

the lesions are well-differentiated, they are frequently isointense, while if the lesions are moderately to poorly differentiated, they might be more often hyperintense (Mulé et al., 2020). In dynamic sequences, lesions less than 2 cm can reveal homogeneous intense enhancement during the arterial phase, whereas larger lesions more often demonstrate heterogeneous enhancement (Hong et al., 2021). HCC will show rapid washout during the portal venous, becoming hypointense relative to the liver (Hong et al., 2021). This rapid washout in which the lesion becomes hypointense relative to adjacent parenchyma on delayed postcontrast images has been reported as an imaging predictive feature of HCC since regenerative and dysplastic nodules do not typically display this finding (Hong et al., 2021; Min et al., 2020). Another predictive imaging finding that increases the HCC suspicion is tumor capsule which can be identified in lesions of any size, but because of increasing capsule thickness with increasing tumor size, capsules can be better observed with larger HCCs (Yang et al., 2022a). Several series indicated that capsule have been observed in 10%–78% of lesions in various series (Liang et al., 2022; Yang et al., 2022; Ye et al., 2019). Typically, they are thin and discontinuous, at T1 and T2-weighted sequences, normally are hypointense, and show progressive delayed enhancement, which are two of the most important factors to HCC diagnosis (Ye et al., 2019).

1.3.1. MRI LI-RADS Classification

Liver Imaging Reporting And Data System (LI-RADS) provides a dynamic and comprehensive system for standardizing the terminology, method, interpretation, and data collection in abnormal liver lesions (Liang et al., 2022). It was designed by a multidisciplinary, international board in order to improve communication, education, patient care and research (Liang et al., 2022).

LI-RADS can be applied to Ultrasound (CEUS - Contrast-Enhanced Ultrasound) and multiphase Computer Tomography (CT) or MRI performed with extracellular contrast agents or hepatobiliary contrast agents in patients with cirrhosis (Liang et al., 2022). Nevertheless, CT/MRI LI-RADS® Diagnostic should not be used in patients < 18 years old (because of potential false-positive results), and in the cases of cirrhosis caused by congenital hepatic fibrosis or vascular disorders (e.g., hereditary haemorrhagic

telangiectasia, Budd-Chiari syndrome, diffuse nodular regenerative hyperplasia, chronic portal vein occlusion or cardiac congestion). The major CT/MRI features indicative of HCC include nonrim APHE, nonperipheral portal venous or delayed phase washout, enhancing capsule appearance, size ≥ 1 cm, and threshold growth by $\geq 50\%$ in ≤ 6 months (Liang et al., 2022). Additionally, there are ancillary features (AF) such as restricted diffusion, corona enhancement, mosaic architecture, that can be applied to help categorize lesions, in order to upgrade (≥ 1 AF favoring malignancy) or downgrade (≥ 1 AF favoring benignity). After LI-RADS analysis, the liver lesion can be classified into one of eight LI-RADS categories that suggest the probability of HCC (figure 4). Figure 5 summarizes the eight LI-RADS categories and the recommended approaches (Liang et al., 2022).

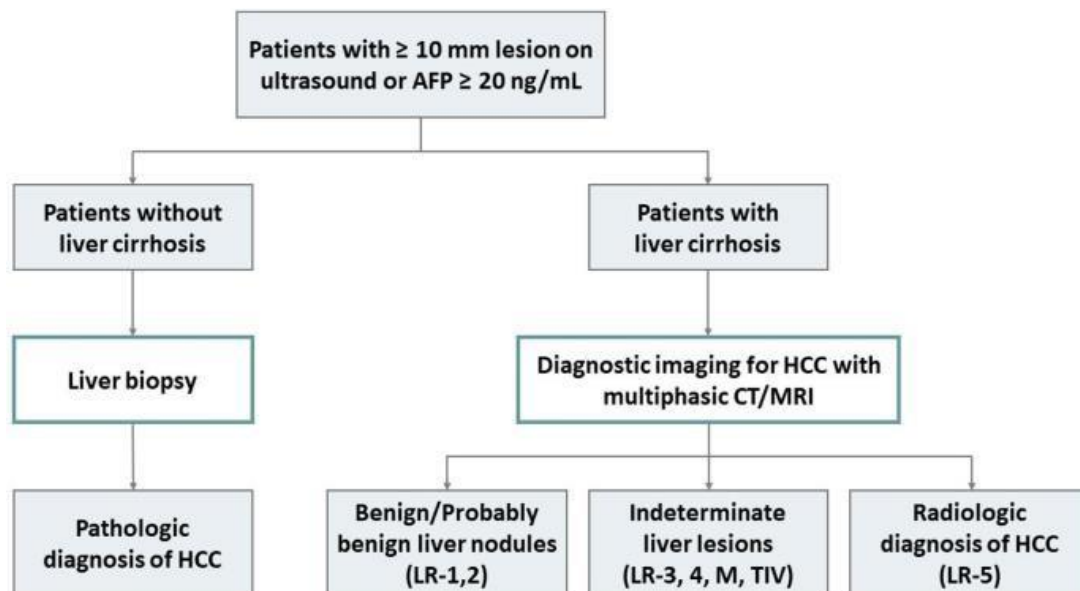


Figure 4 - CT/MRI Diagnostic algorithm. Once the patients have clinical suspicion of HCC or liver lesions ≥ 10 mm or AFP ≥ 20 ng/mL, multiphasic CT or MRI is recommended as the first imaging method for patients with cirrhosis. If the patients doesn't have cirrhosis or for whom HCC diagnosis remains indeterminate on imaging, liver biopsy should be performed to have a definite diagnosis (Liang et al., 2022).

Diagnostic Category	CT/MRI Criteria	Management Recommendation
LR-NC: <i>Noncategorizable</i>	Cannot be categorized because of image degradation or omission	Repeat or alternative diagnostic imaging in ≤3 months
LR-1: <i>Definitely benign</i> 0% HCC 0% malignancy	Simple cyst, solid nodule with characteristics features of hemangioma	Return to surveillance in 6 months
LR-2: <i>Probably benign</i> 13% HCC 14% malignancy	<20 mm with no major features, LR-M features, or ancillary features favoring malignancy	Return to surveillance in 6 months <i>OR</i> Consider repeat diagnostic imaging in ≤6 months
LR-3: <i>Intermediate probability of HCC</i> 38% HCC 40% malignancy	Nonrim APHE <i>AND</i> : • <20 mm with no additional major features No APHE <i>AND</i> : • <20 mm with ≤1 additional major feature <i>OR</i> • ≥20 mm with no additional major features	Repeat or alternative diagnostic imaging in 3-6 months
LR-4: <i>Probably HCC</i> 74% HCC 80% malignancy	Nonrim APHE <i>AND</i> : • <10 mm with ≥1 additional major feature <i>OR</i> • 10-19 mm with enhancing capsule appearance and no other major features <i>OR</i> • ≥20 mm with no additional major features No APHE <i>AND</i> : • <20 mm with ≥2 additional major features <i>OR</i> • ≥20 mm with ≥1 additional major feature	Multidisciplinary discussion for tailored workup • May include biopsy
LR-5: <i>Definitely HCC</i> 94% HCC 97% malignancy	Nonrim APHE <i>AND</i> : • 10-19 mm with nonperipheral washout <i>OR</i> • 10-19 mm with threshold growths <i>OR</i> • ≥20 mm with ≥1 additional major feature	HCC confirmed • Multidisciplinary discussion for consensus management
LR-M: <i>Probably or definitely malignant, not specific for HCC</i> 36% HCC 93% malignancy	Targetoid mass: • Rim APHE • Peripheral washout • Delayed central enhancement • Targetoid diffusion restriction • Targetoid transitional phase or hepatobiliary phase signal intensity Nontargetoid mass not meeting LR-5 criteria <i>AND</i> no TIV, with ≥1 of the following: • Infiltrative appearance • Marked diffusion restriction • Necrosis or severe ischemia • Other feature suggesting non-HCC malignancy	Multidisciplinary discussion for tailored workup • Often includes biopsy
LR-TIV: <i>Malignancy with TIV</i> 79% HCC 92% malignancy	Unequivocal enhancing soft tissue in vein, regardless of visualization of parenchymal mass	Multidisciplinary discussion for tailored workup • May include biopsy

Figure 5 - The eight categories of LI-RADS and each approach (Liang et al., 2022).

In this study was used as a major and AF of HCC: nonrim APHE, nonperipheral portal venous or delayed phase washout, enhancing capsule appearance, diffusion restriction, arterial enhancement, infiltrative appearance, the presence, integrity and enhancement of the capsule, Mild-moderate T2 hyperintensity, Hepatobiliary phase hypointensity and non-smooth tumour margin.

2. Materials and Methods

2.1. Patients and Methods

This retrospective study was authorized by the ethics committee of the Hospital. All the files used in this study were archived and analyzed in a Picture Archiving and Communication System (PACS).

The database was reviewed from January 2017 to January 2022 for patients with MRI with HCC diagnosis who were submitted to surgical treatment. Inclusion criteria were the following: (1) liver MRI protocol examination including arterial, venous, and hepatobiliary phase (HBP) with hepatocyte-specific or extracellular contrast performed at Hospital Santa Maria, Centro Hospitalar Universitário Lisboa Norte, Lisbon, Portugal, before surgery, (2) full histologic description available in the pathologic reports confirming HCC diagnosis of the surgical specimen; and (3) patients without a history of previous HCC treatment. Exclusion criteria were the following: (1) inadequate MR studies to analyze, (2) histopathology not referring presence or absence of MVI, (3) All transplant patients, because they have undergone surgery in another institution; (4) All patients who were subjected to ablative therapies because it was impossible to confront them with the pathological anatomy. Biological and clinical information from population was collected, including: gender, age, laboratorial results (alfa-fetoprotein), and the presence of cirrhosis.

2.2. Image analysis and MRI Protocol

Concerning the MRI Protocol, a preoperative MRI examination was performed on a 1,5 and 3.0 Tesla scanner (Phillips Intera Achieva® 1,5 and 3,0 Tesla) with an 18-channel phased-array body coil and spine coil. All patients were asked to fast for 6–8 h before examination. In all patients, the following breath-hold transversal sequences were conducted: (1) T2- weighted (T2W) turbo spin echo: time of repetition (TR) =2,160 ms, time of echo (TE) =100 ms, the field of view (FOV) = 43 cm × 43 cm, slice thickness = 6 mm. (2) T1-weighted turbo field echo (TFE) in phase. (3) T1-weighted turbo field echo (TFE) out phase. (4) T1-weighted pre-contrast and enhanced sequences [arterial phase

(AP), portal venous phase (PVP), and hepatobiliary phase (HBP)]: TR=3.95 ms, TE=1.92 ms, FOV=40 cm × 40 cm, slice thickness =2 mm. A standard dose (0.025 mmol/kg) of gadoxetic acid disodium (Primovist® - Bayer Schering Pharma AG, Berlin, Germany) or extracellular contrast (Dotarem® - Guerbet Pharma, Paris, France; and Gadovist - Bayer Schering Pharma AG, Berlin, Germany) were intravenously injected at a rate of 2.0 mL/s via a dual power injector, followed by a 30 mL saline flush at the same rate. Bolus tracking in abdominal aorta was performed in order to ensure all three phases were correctly applied to determine the imaging delay time of AP, and then AP was acquired accordingly. Thereafter, PVP, TP, and HBP images were obtained in 90 seconds, 180 seconds, and 20 minutes after contrast material administration, respectively. All images were sent to the picture archiving and communications system (PACS) to be interpreted at workstations.

The images were reviewed by one medical student (observer 1) from 6th grade, and two radiologists, the first one was a 4th year resident (Observer 2) and the second one was a senior physician with 8 years of experience in abdominal radiology (Observer 3). The observers independently reviewed examinations at two different times with an interval of 2 weeks. All radiologic images were evaluated for the following features: (1) the number of lesions was assessed and identified during radiologic assessment according to the BCLC algorithm (solitary vs. 2–3 and over 3 tumours) (Galle et al., 2018); (2) the presence or absence of major and ancillary features MRI features used in LI-RADS CT/MRI® Diagnostic version 2018 which were already mentioned previously; (3) other MRI features, including complete vs. disrupted tumor capsule, and non-smooth tumour margin, (4) the dynamic performance of the tumors during contrast images (arterial hypervascular enhancement and washout behavior), (5) Each nodule was observed and analyzed in axial planes to measure maximum diameter on portal and hepatobiliary axial phase.

2.3. Histopathologic Analysis

All the histopathology data were obtained and consulted in clinical records at the Hospital Santa Maria, Centro Hospitalar Lisboa Norte, Lisbon. Several characteristics were collected, such as tumor dimension, pathological grade, pattern, differentiation tumor, perineural invasion, vascular invasion, characteristic of the borders, and tumor markers in order to evaluate the MVI in HCC patients.

2.4. Statistical data

Considering the small sample size, the median was used in descriptive analysis and non-parametric tests with independency of samples to assess the significance of the difference between groups. Followed by the Shapiro-Wilk test to check the normality of the distribution of the variables cited before with $p < 0.05$ (2-tailed) (table 2). Considering one small sample size, we used the mean, standard deviation in our descriptive analysis of continuous variables and non-parametric tests.

The Kruskal-Wallis test was used to compare age. Fisher's exact test was used to compare gender and imaging findings between groups. Additionally, logistic regression was performed for multivariable analysis of imaging predictors of microvascular invasion, using t-test evaluation. Interobserver and intraobserver variability were calculated with an intraclass correlation coefficient test regarding the differences between the observers and in repeated measurements by the same observer. All the analyzes were performed by using IBM SPSS Statistics for Windows, version 26 (IBM Corp., Armonk, N.Y., USA). A $p < 0.05$ (2-tailed) was chosen as the significance value for all tests.

3. Results and Discussion

3.1. Group Characterisation

In this study, 32 patients with imagological diagnosis of HCC were submitted to surgical resection surgery. Of these, 1 had a relapse of HCC, 3 did not have a full histologic description of surgical specimen available, 3 did not have preoperative imaging performed, and 3 had inadequate imaging studies or poor image quality and were excluded, thus allowing the analysis in 22 patients and 24 lesions.

Concerning the distribution by gender, 74% of the patients were men and 16% were women. Considering the age at the moment of MRI and at the moment of Surgery, the patients averaged 65 years of age. The mean age of patients at the moment of MRI was approximately 70 years with MVI, and 62 years without MVI. The mean age at the moment of Surgery was 71 years with MVI, and 63 years without MVI. Regarding the mean and maximum of days between MRI and Surgery was 115 days and 272 days, respectively.

In this study, 59% (13 patients) were identified with chronic liver disease (CLD) and 41% (9 patients) without CLD. Moreover, 13% of patients with CLD had MVI and 25% without CLD did not have MVI. Additionally, 23% without CLD had MVI, whereas 40% with CLD did not have MVI.

Concerning the elevation of alpha-fetoprotein, which is the laboratory data with the most evidence of MVI in HCC, 58% had high levels and 42% within reference levels. 33% of the patients presented high Alpha fetoprotein levels with MVI, however 38% of the patients with high alpha fetoprotein levels did not have MVI. On the other hand, 8% of the patients with alpha fetoprotein within reference values had MVI, and 21% did not have MVI. The characterization of the patients is shown in table 1.

After testing the existence of normality in all variables figured in table 2, all presented p value <0.05, so these variables did not have normal distributions.

Table 1 - Baseline patient characteristics and by group according MVI in biopsy

	Total of lesions* N= 24 (22 patients)	Lesions with MVI	
		Yes N= 11	No N= 13
Age at the moment of MRI, n (%)**	64,82 ± 11,27 [29-79]	70,57	62,01
Age at the moment of Surgery, n (%)**	65,05 ± 11,27 [29-79]	71,36	63,22
Gender, N (%)			
Male	16 (73%)	7	10
Female	6 (27%)	3	4
Chronic liver disease, n (%)			
Yes	13 (59%)	3 (13%)	10 (40%)
No	9 (41%)	6 (25%)	5 (23%)
Alpha fetoprotein, n (%):			
Elevated	14 (58%)	8 (33%)	9 (38%)
Normal	10 (42%)	2 (8%)	5 (21%)

*Two patients had two independent lesions analyzed. **Mean ± standard deviation (SD) and minimum and maximum.

Table 2 - Shapiro-Wilk Normality test

Shapiro-Wilk	Statistic	Number	p-value
Sex	0,561	22	0,000
Age at the moment of MRI	0,876	22	0,010
Age at the moment of Surgery	0,872	22	0,008
Number of days between MRI and Surgery	0,893	22	0,022

3.2. Analysis of MRI features as predictors of MVI

In this section, several statistical tests were performed to determine if any of the MRI features correlate with MVI pathology in each data reading from each observer. All observers were aware that the patients had HCC but were blinded to all the other information, including clinical history, and MVI findings on pathology.

All variables were equally distributed by each observer to perform the statistical tests to compare and explore inter and intra-observation correlations and differences.

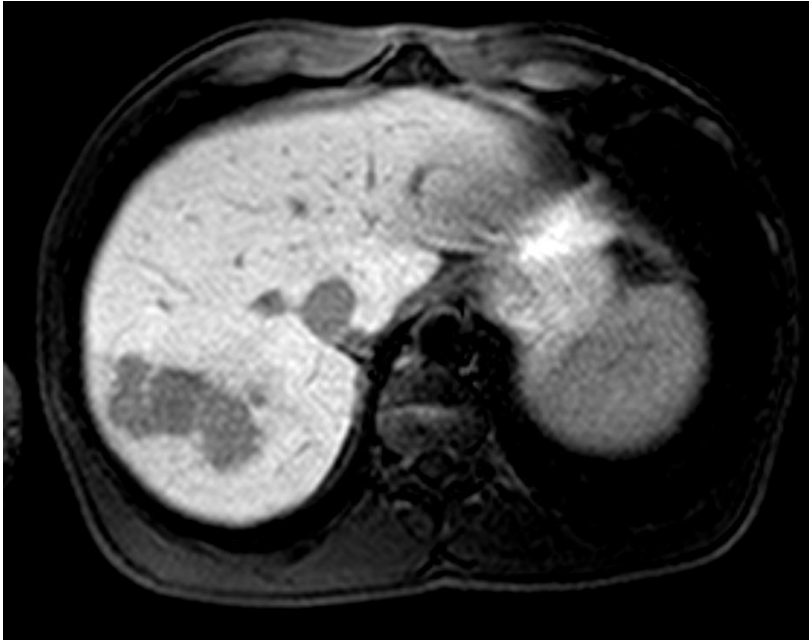


Figure 7 - Axial plane T1 fat saturation with HBP contrast showing hypointensity lesion. Hypointensity with HBP contrast is an MRI feature of MVI in HCC. This image is showing heterogeneity enhancement, lack of capsule and irregularity of borders.

3.2.1. Reliability of MRI Features analysis interobserver

In this section, all variables used in this study were statistically analyzed for each observer. Firstly, reliability interobserver were performed in order to find statistical differences between observers. Then, T-students and fisher exact test analysis were made to study if MRI features were predictors of MVI. Ultimately, the interobserver reliability was evaluated to get consistency in the results.

In table 4, the size of each lesion measured in a portal or an HBP on the axial plane demonstrated excellent reliability among the observers which is supported by literature (Liang et al., 2022). All the ROI measured in this study, in T1 in-phase and out-phase sequences, and in T2 sequence showed exceptional consistency. These results showed that the observers used similar methods to measure the lesions on the axial plane.

The solidity of the results among the observers in the T2 sequence signal intensity was only moderate. The moderate reliability of this result can be attributed to different observer assessment, providing variability and a decrease in reliability of the test.

Of the remaining variables, specifically on washout, capsule integrity, and peritumoral enhancement, the impact of dependent observer evaluation may have influenced the results.

Table 3 - Intraclass correlation coefficient test to evaluate interobserver variability.

Intraclass Correlation Coefficient*	
Size in portal axial phase	0,994 (0,963-0,991)
Size in hepatobiliary axial phase	0,966 (0,919-0,988)
ROI T1 in-phase sequence	0,987 (0,974-0,994)
ROI T1 out-phase sequence	0,987 (0,972-0,994)
ROI T2 sequence	0,991 (0,983-0,996)
Signal in T2 sequence	0,777 (0,558-0,896)
Restriction in diffusion sequence	0,854 (0,698-0,936)
Hypervascularity lesion	0,644 (0,174-0,850)
Washout	0,348 (-0,352-0,712)
Capsule	0,724 (0,439-0,877)
Peritumoral enhancement	0,413 (-0,052-0,717)
Margins of the lesion in MRI	0,789 (0,582-0,902)

*Confidence of the interval used was 95%. Average measures and Lower and Upper bound.

3.2.2. Analysis of predictors of MVI in Observer 1, 2 and 3

In table 5, only the lesions with MVI were evaluated. The size of the lesions in HBP exhibited statistically significant results (even if the first one was borderline), demonstrating a relationship between this variable and MVI. Some studies supported this evidence, indicating that the size of the lesions is an important MRI feature predictor of MVI. The HBP (Tang, 2020; L. Zhang et al., 2020) had a more significant result (p 0.039) in comparison with the portal phase, demonstrating the importance and specificity of the hepatocyte-specific contrast (Renzulli et al., 2016) in better defining the lesions. The washout demonstrated as well statistical significance (p 0,038) as an MVI predictor. This result was confirmed in the literature and perhaps can explain the importance of angiogenesis in carcinogenesis (Shirabe et al., 2014).

The other features didn't exhibit statistical significance. These results contradict some studies which support the importance of these variables as predictors of MVI (Lee et al., 2017), however, other studies also demonstrated inconsistency (Lee et al., 2017).

In observer 2, only the measure of the size of the lesion in the portal axial phase revealed $p < 0,05$ ($p = 0,037$), demonstrating once again the importance of the size of the lesions in MVI which is supported by the literature (Lee et al., 2017).

Comparing these results to observer 1, most of the variables didn't exhibit statistical significance. These results could be explained by the dependent observer evaluation which can impact negatively the p-value, and consequently, the importance of the MRI features as predictors of MVI.

In table 7, the measures of MRI features were performed by the physician who had more years of experience. This fact could contribute and impact positively on the results.

The size of the lesions in the portal and HBP phase and the washout measures exhibited statistically significant results, as in observer 1, supporting the results verified in the literature. This analysis demonstrated the importance as well of the T2 signal in MVI, which is supported by the literature. This result could be explained by the composition of malignancy lesions which were composed by a high percentage of water (Lee et al., 2017).

In summary, the importance of the Portal phase, HBP, Washout and Hypervascularity as a features predictor of MVI were observed. Observers 1 and 3 demonstrated the importance of HBP and Washout as MRI feature predictors in MVI. The relevance of Portal phase was showed on observer 2 and 3. Observer 3 proved the importance of Hypervascularity as MRI feature predictor in MVI. All these results were supported by the literature (Lee et al., 2017). The other variables evaluated in this study didn't demonstrate the same relevance as the predictor of MVI presented in other studies (Hong et al., 2021).

Table 4 - All metrics obtained with t-test analysis for comparison between MRI features and MVI in biopsy in observer 1. Significant values are considered for $p < 0.05$. Significant changes are exhibited in bold. Equal variances were assumed after Levene's test with $p > 0.05$.

Independent Samples Test – T-test		p-value
Size in portal axial phase	Equal variances assumed	0,052
Size in hepatobiliary axial phase	Equal variances assumed	0,039
ROI T1 In-phase sequence	Equal variances assumed	0,502
ROI T1 out-phase sequence	Equal variances assumed	0,325
ROI T2 sequence	Equal variances assumed	0,937
Signal in T2 sequence	Equal variances assumed	0,813
Restriction in diffusion sequence	Equal variances assumed	0,732
Hypervascularity lesion	Equal variances assumed	0,539
Washout	Equal variances assumed	0,038
Capsule	Equal variances assumed	0,260
Peritumoral enhancement	Equal variances assumed	0,624
Margins of the lesion in MRI	Equal variances assumed	0,785

Table 5- All metrics obtained with t-test analysis for comparison between MRI features and MVI in biopsy in observer 2. Significant values are considered for $p < 0.05$. Significant changes are exhibited in bold. Equal variances were assumed after Levene's test with $p > 0.05$.

Independent Samples Test – T-test		p-value
Size in portal axial phase	Equal variances assumed	0,037
Size in hepatobiliary axial phase	Equal variances assumed	0,153
ROI T1 In-phase sequence	Equal variances assumed	0,412
ROI T1 out-phase sequence	Equal variances assumed	0,339
ROI T2 sequence	Equal variances assumed	0,928
Signal in T2 sequence	Equal variances assumed	0,767
Restriction in diffusion sequence	Equal variances assumed	0,572
Hypervascularity lesion	Equal variances assumed	0,193
Washout	Equal variances assumed	0,092
Capsule	Equal variances assumed	0,865
Peritumoral enhancement	Equal variances assumed	0,440
Margins of the lesion in MRI	Equal variances assumed	0,151

Table 6 - All metrics obtained with t-test analysis for comparison between MRI features and MVI in biopsy in observer 3. Significant values are considered for $p < 0.05$. Significant changes are exhibited in bold. Equal variances were assumed after Levene's test with $p > 0.05$.

Independent Samples Test – T-test		p-value
Size in portal axial phase	Equal variances assumed	0,043
Size in hepatobiliary axial phase	Equal variances assumed	0,046
ROI T1 In-phase sequence	Equal variances assumed	0,390
ROI T1 out-phase sequence	Equal variances assumed	0,432
ROI T2 sequence	Equal variances assumed	0,992
Signal in T2 sequence	Equal variances assumed	0,087
Restriction in diffusion sequence	Equal variances assumed	0,608
Hypervascularity lesion	Equal variances assumed	0,050
Washout	Equal variances assumed	0,600
Capsule	Equal variances assumed	0,204
Peritumoral enhancement	Equal variances assumed	0,650
Margins of the lesion in MRI	Equal variances assumed	0,940

3.2.3. Reliability of MRI Features analysis intraobserver

In order to find out the consistency or/and the differences of the measures in each observer, the reliability was analyzed with intraclass correlation coefficient. For most of the variables analyzed by each observer, it was possible to determine that there was a good or excellent consistency in the evaluation of each variable. This fact demonstrated the consistency of data reading by each observer (table 7, 8 and 9).

Table 7 - Intraclass correlation coefficient test to evaluate intraobserver 1 variability.

Intraclass Correlation Coefficient*	
Size in portal axial phase	0,996 (0,981-0,997)
Size in hepatobiliary axial phase	0,988 (0,934-0,996)
ROI T1 in-phase sequence	0,999 (0,998-1,000)
ROI T1 out-phase sequence	1,000 (0,997-1,000)
ROI T2 sequence	0,999 (0,998-1,000)
Signal in T2 sequence	0,972 (0,921-0,994)
Restriction in diffusion sequence	1,000 (0,999-1,000)
Hypervascularity lesion	1,000 (0,999-1,000)
Washout	0,954 (0,853-0,983)
Capsule	1,000 (0,998-1,000)
Peritumoral enhancement	0,997 (0,994-0,999)
Margins of the lesion in MRI	0,930 (0,889-0,978)

*Confidence of the interval used was 95%. Average measures and Lower and Upper bound.

Table 8 - Intraclass correlation coefficient test to evaluate intraobserver 2 variability.

Intraclass Correlation Coefficient*	
Size in portal axial phase	0,997 (0,992-0,999)
Size in hepatobiliary axial phase	0,994 (0,976-0,998)
ROI T1 in-phase sequence	0,979 (0,950-0,992)
ROI T1 out-phase sequence	0,979 (0,942-0,992)
ROI T2 sequence	0,994 (0,987-0,998)
Signal in T2 sequence	0,772 (0,467-0,902)
Restriction in diffusion sequence	1,000 (0,999-1,000)
Hypervascularity lesion	1,000 (0,999-1,000)
Washout	0,937 (0,848-0,974)
Capsule	0,999 (0,997-1,000)
Peritumoral enhancement	0,712 (0,293-0,882)
Margins of the lesion in MRI	0,960 (0,940-0,993)

Table 9 - Intraclass correlation coefficient test to evaluate intraobserver 3 variability.

Intraclass Correlation Coefficient*	
Size in portal axial phase	0,998 (0,996-0,999)
Size in hepatobiliary axial phase	0,999 (0,998-0,999)
ROI T1 in-phase sequence	0,999 (0,998-1,000)
ROI T1 out-phase sequence	0,991 (0,982-0,998)
ROI T2 sequence	0,994 (0,987-0,998)
Signal in T2 sequence	0,999 (0,996-1,000)
Restriction in diffusion sequence	1,000 (0,999-1,000)
Hypervascularity lesion	1,000 (0,999-1,000)
Washout	0,998 (0,996-0,999)
Capsule	0,999 (0,998-1,000)
Peritumoral enhancement	0,712 (0,293-0,882)
Margins of the lesion in MRI	0,808 (0,556-0,917)

3.2.4. Microvasculature invasion predicted by MRI features

In order to determine if some of the variables analyzed in this study could predict MVI, logistic regression was made. Observer 3's analysis was selected because of his years of experience in the field. The variables statistically significant (p-value <0,05) were analyzed to predict MVI.

In Table 10, the results obtained didn't seem to demonstrate that the variables under study can predict microvascular invasion, because they do not present a statistically significant result (p-value 0,08), even if they were statistically significant independently. These results may perhaps be explained, due to the insufficient population sample in the test, because for this analysis to be statistically significant it would be necessary to have a larger sample for each variable.

Table 10 - MVI prediction by MRI features

Variables	Score	p-value
Size in portal axial phase	4.879	0.027
Size in hepatobiliary axial phase	4.200	0.040
Hypervascularity lesion	2.637	0.104
Overall Statistics	6.761	0.080

4. Limitations and Futures Perspectives

This study, just like other researches, has undeniable limitations, such as the retrospective type of study and the small size of the population. It would be desirable to carry out prospective research and with a larger number of individuals to confirm and obtain robust results. Due to the organization of the national health service, most of the cases of HCC requiring liver transplantation were transferred to another hospital, and the remaining tests were performed in that hospital. Secondly, some exams didn't have all sequences, as expected. The MRI protocol over the years has undergone some changes. Since this study was retrospective, it was natural that not all exams had all the same exact sequences proposed and in use in the current protocol. Additionally, technical or acquisition errors, such as artifact related to patients motion and breathing may interfere with the study's statistical results. Thirdly, despite having selected samples according to rigorous inclusion and exclusion criteria, selection bias may not be prevented.

The qualitative data were validated by three observers, one medical student, and two physicians with different years of experience in the field. This fact can be cited as one of the possible causes of divergences in some of the least expected results. No other studies based on MRI features and MVI, to the best of our knowledge, have been published before using a medical student as an observer. Additionally, another positive perspective of this study was the calculation of interobserver and intraobserver differences which, once again, to the best of our knowledge, have not been published before.

Other limitations were identified, such as the ROI measure. The ROI was manually selected from the section with 2/3 of the lesions, which may have influenced the results. However, the same strategy was used in each measurement and in each observer, demonstrating consistency in results.

Another limitation of this study identified was the time between MRI exams and the surgeries, which fluctuate between 19-272 days.

This study did not analyze the follow-up and complications of each surgery which could have impact on general survival.

The p-value employed as a reference for the statistical tests, fixed at 0.05, was not Bonferroni corrected. It was considered that this correction was exceedingly conservative and it was impossible to exclude the dependence of variables, which could have resulted in a large number of false negatives as well.

In future studies, in order to alleviate and to improve or obtain more robust results, larger data set will be needed to evaluate the model more robustly, the contrast should be always hepatocyte-specific contrast, tumoral markers, more laboratory data as well as overall survival and disease-free survival should be used.

5. Conclusions

Throughout the literature, most of the studies conducted so far have been obtained in Asian countries, which gives an epidemiological difference in the etiology of HCC. In Asian countries, most HCCs have HBV or HBC as a risk factor, while in Europe, the vast majority are due to HBC followed by alcohol consumption. Considering that this study was obtained from a small sample from a hospital in Portugal, this gives another perspective on the evaluation of HCC which may be similar to the rest of Europe.

This study aimed to verify the importance of the role of MRI in predicting the MVI on HCC and in patient stratification. Additionally, MRI features may directly or indirectly reveal underlying structures as in histopathology such as the size, capsule, and peritumoral involvement in order to predict or validate the MVI in HCC patients. Therefore, this strategy may provide helpful preoperative knowledge valuable to establishing a treatment strategy. Moreover, during the monitoring and follow-up of HCC during and after treatment, this application may also offer a non-invasive alternative to predict MVI on HCC.

In regards to data analysis, Interobserver variability was calculated regarding the observance of the differences in the measurements between observers. Most of the measurements indicated excellent reliability, $>0,900$, such as the size of the lesions in the portal and hepatobiliary phase, ROI T1 in and out-phase, and RO in the T2 sequence. Additionally, good reliability (between $0,700$ and $0,900$) was obtained as well, such as in the evaluation of the T2 signal, restriction diffusion sequence, and margins of the lesion.

Secondly, all measurements of MRI features were estimated to determine if they were predictors of MVI. This evaluation was made for each observer and analyzed individually, then the results were compared among the observers. All observers demonstrated the importance of the portal phase as an MRI feature predictor of MVI. Moreover, observers 1 and 3 revealed the importance of HBP and Washout as MRI feature predictors in MVI.

The intraobserver variability was calculated in order to find differences in the two repeated measurements by the same observer, which demonstrated excellent reliability.

In the last evaluation, in an attempt to verify whether MVI could be predicted by MRI features in this study, the variables selected were unable to predict MVI in each lesion.

Some of the results observed in this study are in line with the literature, however, other results are inconsistent with the literature.

This study shows that we may have some predictive features of MVI, although they may differ among those analyzing the images because there are some inconsistencies in the methods of analysis. More studies are required, with better parameters and clinical correlation, preferably prospective and with larger populations, to try to establish MR predictors of MVI to help better identify and guide patients with MVI.

6. Acknowledgments

This dissertation is the result of dedication and continuous effort and could not have been undertaken without the support of many members. Firstly, I would like to thank my advisor, Professor Doctor Sofia Pereira Coutinho Reimão, for the opportunity and self-determination she has provided. I am sure, with the guidance she has given me, that I am ready to continue my long journey in this wonderful field. I would like to thank Dr. Maria Inês for her tireless help and companionship, she has shown me that persistence, competence, and patience are indispensable values in this area. I would also like to thank Dr. Carlos Mendonça for his time, effort, passion and advice in the realization of this study. Their genuine fascination and enthusiasm for the pursuit of knowledge will forever stay with me. I would like to thank Dra. Carla Guerreiro for her help and insight when I most needed it. She was an outstanding and fundamental piece in this study.

I must express my gratitude to some of my friends who have always supported me. I would like to thank Christopher for all the support he gave me, for his resilience, and for always being there for me. I would like to thank two other people who represent everything I am right now, my grandmother Emilia Serrano and my lovely cousin Lita Pedrosa. Lastly, I am indebted to my lovely fiancée, Ana Resendes, for all her love, help, and insight.

7. References

- Ahn, J. C., Teng, P. C., Chen, P. J., Posadas, E., Tseng, H. R., Lu, S. C., & Yang, J. D. (2021). Detection of Circulating Tumor Cells and Their Implications as a Biomarker for Diagnosis, Prognostication, and Therapeutic Monitoring in Hepatocellular Carcinoma. *Hepatology (Baltimore, Md.)*, *73*(1), 422–436. <https://doi.org/10.1002/HEP.31165>
- Ahn, S. J., Kim, J. H., Park, S. J., Kim, S. T., & Han, J. K. (2019). Hepatocellular carcinoma: preoperative gadoxetic acid–enhanced MR imaging can predict early recurrence after curative resection using image features and texture analysis. *Abdominal Radiology*, *44*(2), 539–548. <https://doi.org/10.1007/s00261-018-1768-9>
- An, C., Kim, D. W., Park, Y. N., Chung, Y. E., Rhee, H., & Kim, M. J. (2015). Single Hepatocellular Carcinoma: Preoperative MR Imaging to Predict Early Recurrence after Curative Resection. <https://doi.org/10.1148/Radiol.15142394>, *276*(2), 433–443. <https://doi.org/10.1148/RADIOL.15142394>
- Cabrera, R., & Nelson, D. R. (2010). Review article: The management of hepatocellular carcinoma. *Alimentary Pharmacology and Therapeutics*, *31*(4), 461–476. <https://doi.org/10.1111/j.1365-2036.2009.04200.x>
- Clark, T., Maximin, S., Meier, J., Pokharel, S., & Bhargava, P. (2015). Hepatocellular Carcinoma: Review of Epidemiology, Screening, Imaging Diagnosis, Response Assessment, and Treatment. *Current Problems in Diagnostic Radiology*, *44*(6), 479–486. <https://doi.org/10.1067/j.cpradiol.2015.04.004>
- Darren, J., Cheng, H., Snow, Y., Xin, H., Phoebe, T., Wen, H., Margaret, T., Grace, L., Jie, N. (2022). Clinical characteristics, surveillance, treatment allocation, and outcomes of non-alcoholic fatty liver disease-related hepatocellular carcinoma: a systematic review and meta-analysis. *Lancet Oncology*, *23* (10), 521-30. [https://doi.org/10.1016/S1470-2045\(22\)00078-X](https://doi.org/10.1016/S1470-2045(22)00078-X)
- Desai, A., Sandhu, S., Lai, J. P., & Sandhu, D. S. (2019). Hepatocellular carcinoma in non-cirrhotic liver: A comprehensive review. *World Journal of Hepatology*, *11*(1), 1–18. <https://doi.org/10.4254/WJH.V11.I1.1>

- Dimitroulis, D., Damaskos, C., Valsami, S., Davakis, S., Garmpis, N., Spartalis, E., Athanasiou, A., Moris, D., Sakellariou, S., Kykalos, S., Tsourouflis, G., Garmpi, A., Delladetsima, I., Kontzoglou, K., & Kouraklis, G. (2017). From diagnosis to treatment of hepatocellular carcinoma: An epidemic problem for both developed and developing world. *World Journal of Gastroenterology*, 23(29), 5282–5294. <https://doi.org/10.3748/wjg.v23.i29.5282>
- European Association for the Study of the Liver. EASL Policy Statement on Liver Cancer Screening. https://easl.eu/wp-content/uploads/2022/05/policy-statement-on-liver-cancer-screening_31May2022.pdf
- Fattovich, G., Stroffolini, T., Zagni, I., & Donato, F. (2004). Hepatocellular carcinoma in cirrhosis: Incidence and risk factors. *Gastroenterology*, 127(5 SUPPL.). <https://doi.org/10.1053/j.gastro.2004.09.014>
- Fitzmaurice, C., Akinyemiju, T., Abera, S., Ahmed, M., Alam, N., Alemayohu, M. A., Allen, C., Al-Raddadi, R., Alvis-Guzman, N., Amoako, Y., Artaman, A., Ayele, T. A., Barac, A., Bensenor, I., Berhane, A., Bhutta, Z., Castillo-Rivas, J., Chitheer, A., Choi, J. Y., ... Naghavi, M. (2017). The Burden of Primary Liver Cancer and Underlying Etiologies From 1990 to 2015 at the Global, Regional, and National Level: Results From the Global Burden of Disease Study 2015. *JAMA Oncology*, 3(12), 1683. <https://doi.org/10.1001/JAMAONCOL.2017.3055>
- Galle, P. R., Forner, A., Llovet, J. M., Mazzaferro, V., Piscaglia, F., Raoul, J. L., Schirmacher, P., & Vilgrain, V. (2018). EASL Clinical Practice Guidelines: Management of hepatocellular carcinoma. *Journal of Hepatology*, 69(1), 182–236. <https://doi.org/10.1016/J.JHEP.2018.03.019>
- Hartke, J., Johnson, M., & Ghabril, M. (2017). The diagnosis and treatment of hepatocellular carcinoma. *Seminars in Diagnostic Pathology*, 34(2), 153–159. <https://doi.org/10.1053/J.SEMDP.2016.12.011>
- He, Y. Z., He, K., Huang, R. Q., Wang, Z. L., Ye, S. W., Liu, L. W., Luo, Q. J., & Hu, Z. M. (2020). Preoperative evaluation and prediction of clinical scores for hepatocellular carcinoma microvascular invasion: a single-center retrospective analysis. *Annals of Hepatology*, 19(6), 654–661. <https://doi.org/10.1016/j.aohep.2020.07.002>

- Hong, S. B., Choi, S. H., Kim, S. Y., Shim, J. H., Lee, S. S., Byun, J. H., Park, S. H., Kim, K. W., Kim, S., & Lee, N. K. (2021). MRI Features for Predicting Microvascular Invasion of Hepatocellular Carcinoma: A Systematic Review and Meta-Analysis. *Liver Cancer, 10*(2), 94–106. <https://doi.org/10.1159/000513704>
- Kim, D. H., Choi, S. H., Lee, J. S., & Choi, J. il. (2022). Inter-reader agreement of abbreviated magnetic resonance imaging for hepatocellular carcinoma detection: a systematic review and meta-analysis. *Abdominal Radiology, 47*(1), 123–132. <https://doi.org/10.1007/S00261-021-03297-0/TABLES/3>
- Kojiro, M. (2005). Histopathology of liver cancers. *Best Practice & Research Clinical Gastroenterology, 19*(1), 39–62. <https://doi.org/10.1016/J.BPG.2004.10.007>
- Kraglund, F., Villadsen, G. E., & Jepsen, P. (2023). Effects of Curative-Intent Treatments on Hepatocellular Carcinoma Survival in Alcohol-Related Cirrhosis: A Nationwide Study. *Clinical Epidemiology, 15*, 39–48. <https://doi.org/10.2147/CLEP.S393118>
- Krinsky, G., & Shanbhogue, K. (2021). Proliferative versus nonproliferative hepatocellular carcinoma: Clinical and imaging implications. *Radiology, 300*(3), 583–585. <https://doi.org/10.1148/RADIOL.2021211316/ASSET/IMAGES/LARGE/RADIOL.2021211316.FIG2.JPEG>
- Kulik, L., & El-Serag, H. B. (2019). Epidemiology and Management of Hepatocellular Carcinoma. *Gastroenterology, 156*(2), 477-491.e1. <https://doi.org/10.1053/J.GASTRO.2018.08.065>
- Lee, S., Kim, S. H., Lee, J. E., Sinn, D. H., & Park, C. K. (2017). Preoperative gadoxetic acid-enhanced MRI for predicting microvascular invasion in patients with single hepatocellular carcinoma. *Journal of Hepatology, 67*(3), 526–534. <https://doi.org/10.1016/j.jhep.2017.04.024>
- Lei, Z., Li, J., Wu, D., Xia, Y., Wang, Q., Si, A., Wang, K., Wan, X., Lau, W. Y., Wu, M., & Shen, F. (2016). Nomogram for Preoperative Estimation of Microvascular Invasion Risk in Hepatitis B Virus-Related Hepatocellular Carcinoma Within the Milan

- Criteria. *JAMA Surgery*, 151(4), 356–363.
<https://doi.org/10.1001/JAMASURG.2015.4257>
- Li, Y., Chen, J., Weng, S., Sun, H., Yan, C., Xu, X., Ye, R., & Hong, J. (2019). Small hepatocellular carcinoma: using MRI to predict histological grade and Ki-67 expression. *Clinical Radiology*, 74(8), 653.e1-653.e9.
<https://doi.org/10.1016/J.CRAD.2019.05.009>
- Li, Y., Yan, C., Weng, S., Shi, Z., Sun, H., Chen, J., Xu, X., Ye, R., & Hong, J. (2019). Texture analysis of multi-phase MRI images to detect expression of Ki67 in hepatocellular carcinoma. *Clinical Radiology*, 74(10), 813.e19-813.e27.
<https://doi.org/10.1016/J.CRAD.2019.06.024>
- Liang, X., Shi, S., & Gao, T. (2022). Preoperative gadoxetic acid-enhanced MRI predicts aggressive pathological features in LI-RADS category 5 hepatocellular carcinoma. *Clinical Radiology*, 77(9), 708–716. <https://doi.org/10.1016/j.crad.2022.05.018>
- Llovet, J. M., Kelley, R. K., Villanueva, A., Singal, A. G., Pikarsky, E., Roayaie, S., Lencioni, R., Koike, K., Zucman-Rossi, J., & Finn, R. S. (2021). Hepatocellular carcinoma. *Nature Reviews Disease Primers* 2021 7:1, 7(1), 1–28.
<https://doi.org/10.1038/s41572-020-00240-3>
- Marrero, J. A., Kulik, L. M., Sirlin, C. B., Zhu, A. X., Finn, R. S., Abecassis, M. M., Roberts, L. R., & Heimbach, J. K. (2018). Diagnosis, Staging, and Management of Hepatocellular Carcinoma: 2018 Practice Guidance by the American Association for the Study of Liver Diseases. *Hepatology*, 68(2), 723–750.
<https://doi.org/10.1002/hep.29913>
- McGlynn, K. A., Petrick, J. L., & El-Serag, H. B. (2021). Epidemiology of Hepatocellular Carcinoma. *Hepatology (Baltimore, Md.)*, 73 Suppl 1(Suppl 1), 4–13.
<https://doi.org/10.1002/HEP.31288>
- Min, J. H., Lee, M. W., Park, H. S., Lee, D. H., Park, H. J., Lim, S., Choi, S. Y., Lee, J., Lee, J. E., Ha, S. Y., Cha, D. I., Carriere, K. C., & Ahn, J. H. (2020). Interobserver Variability and Diagnostic Performance of Gadoxetic Acid-enhanced MRI for Predicting

Microvascular Invasion in Hepatocellular Carcinoma. *Radiology*, 297(3), 573–581.
<https://doi.org/10.1148/RADIOL.2020201940>

Mulé, S., Pregliasco, A. G., Tenenhaus, A., Kharrat, R., Amaddeo, G., Baranes, L., Laurent, A., Renault, H., Sommacale, D., Djabbari, M., Pigneur, F., Tacher, V., Kobeiter, H., Calderaro, J., & Luciani, A. (2020). Multiphase liver MRI for identifying the macrotrabecular-massive subtype of hepatocellular carcinoma. *Radiology*, 295(3), 562–571. <https://doi.org/10.1148/radiol.2020192230>

Petrick, J. L., Kelly, S. P., Altekruise, S. F., McGlynn, K. A., & Rosenberg, P. S. (2016). Future of hepatocellular carcinoma incidence in the United States forecast through 2030. *Journal of Clinical Oncology*, 34(15), 1787–1794.
<https://doi.org/10.1200/JCO.2015.64.7412>

Renne, S. L., Sarcognato, S., Sacchi, D., Guido, M., Roncalli, M., Terracciano, L., & di Tommaso, L. (2021). Hepatocellular carcinoma: a clinical and pathological overview. *Pathologica*, 113(3), 203. <https://doi.org/10.32074/1591-951X-295>

Renzulli, M., Brocchi, S., Cucchetti, A., Mazzotti, F., Mosconi, C., Sportoletti, C., Brandi, G., Pinna, A. D., & Golfieri, R. (2016). Can Current Preoperative Imaging Be Used to Detect Microvascular Invasion of Hepatocellular Carcinoma? *Radiology*, 279(2), 432–442. <https://doi.org/10.1148/RADIOL.2015150998>

Sagnelli, E., Macera, M., Russo, A., Coppola, N., & Sagnelli, C. (2020). Epidemiological and etiological variations in hepatocellular carcinoma. *Infection*, 48(1), 7–17.
<https://doi.org/10.1007/s15010-019-01345-y>

Schlageter, M., Terracciano, L. M., D'Angelo, S., & Sorrentino, P. (2014). Histopathology of hepatocellular carcinoma. *World Journal of Gastroenterology*, 20(43), 15955.
<https://doi.org/10.3748/WJG.V20.I43.15955>

Shirabe, K., Toshima, T., Kimura, K., Yamashita, Y., Ikeda, T., Ikegami, T., Yoshizumi, T., Abe, K., Aishima, S., & Maehara, Y. (2014). New scoring system for prediction of microvascular invasion in patients with hepatocellular carcinoma. *Liver International*, 34(6), 937–941. <https://doi.org/10.1111/liv.12459>

- Silva, A. C., Evans, J. M., McCullough, A. E., Jatoi, M. A., Vargas, H. E., & Hara, A. K. (2009). MR imaging of hypervascular liver masses: a review of current techniques. *Radiographics : A Review Publication of the Radiological Society of North America, Inc*, 29(2), 385–402. <https://doi.org/10.1148/RG.292085123>
- Sim, J. Z. T., Hui, T. C. H., Chuah, T. K., Low, H. M., Tan, C. H., & Shelat, V. G. (2022). Efficacy of texture analysis of pre-operative magnetic resonance imaging in predicting microvascular invasion in hepatocellular carcinoma. *World Journal of Clinical Oncology*, 13(11), 918–928. <https://doi.org/10.5306/wjco.v13.i11.918>
- Sung, H., Ferlay, J., Siegel, R. L., Laversanne, M., Soerjomataram, I., Jemal, A., & Bray, F. (2021). Global Cancer Statistics 2020: GLOBOCAN Estimates of Incidence and Mortality Worldwide for 36 Cancers in 185 Countries. *CA: A Cancer Journal for Clinicians*, 71(3), 209–249. <https://doi.org/10.3322/CAAC.21660>
- Tang, A. (2020). Using MRI to assess microvascular invasion in hepatocellular carcinoma. *Radiology*, 297(3), 582–583. <https://doi.org/10.1148/radiol.2020203376>
- Vogel, A., Meyer, T., Sapisochin, G., Salem, R., & Saborowski, A. (2022). Hepatocellular carcinoma. *The Lancet*, 400(10360), 1345–1362. [https://doi.org/10.1016/S0140-6736\(22\)01200-4/ATTACHMENT/EF14ECF6-C0FF-4B55-BE7F-A371A4DB9FBE/MMC1.PDF](https://doi.org/10.1016/S0140-6736(22)01200-4/ATTACHMENT/EF14ECF6-C0FF-4B55-BE7F-A371A4DB9FBE/MMC1.PDF)
- Wang, L., Jia, M., Wen, X., Shen, J., & Yang, H. (2022). Diagnostic value of magnetic resonance imaging features of microvascular invasion in hepatocellular carcinoma: a meta-analysis. *Diagnostic and Interventional Radiology*, 28(5), 428–440. <https://doi.org/10.5152/dir.2022.21108>
- Wang, W., Guo, Y., Zhong, J., Wang, Q., Wang, X., Wei, H., Li, J., & Xiu, P. (2021). The clinical significance of microvascular invasion in the surgical planning and postoperative sequential treatment in hepatocellular carcinoma. *Scientific Reports* 2021 11:1, 11(1), 1–10. <https://doi.org/10.1038/s41598-021-82058-x>
- Xu, P., Zeng, M., Liu, K., Shan, Y., Xu, C., & Lin, J. (2014). Microvascular invasion in small hepatocellular carcinoma: Is it predictable with preoperative diffusion-weighted imaging? *Journal of Gastroenterology and Hepatology (Australia)*, 29(2), 330–336. <https://doi.org/10.1111/jgh.12358>

- Yang, H., Han, P., Huang, M., Yue, X., Wu, L., Li, X., Fan, W., Li, Q., Ma, G., & Lei, P. (2022). The role of gadoxetic acid-enhanced MRI features for predicting microvascular invasion in patients with hepatocellular carcinoma. *Abdominal Radiology*, 47(3), 948–956. <https://doi.org/10.1007/s00261-021-03392-2>
- Ye, Z., Jiang, H., Chen, J., Liu, X., Wei, Y., Xia, C., Duan, T., Cao, L., Zhang, Z., & Song, B. (2019). Texture analysis on gadoxetic acid enhanced-MRI for predicting Ki-67 status in hepatocellular carcinoma: A prospective study. *Chinese Journal of Cancer Research*, 31(5), 806. <https://doi.org/10.21147/J.ISSN.1000-9604.2019.05.10>
- Zech, C. J., Ba-Ssalamah, A., Berg, T., Chandarana, H., Chau, G. Y., Grazioli, L., Kim, M. J., Lee, J. M., Merkle, E. M., Murakami, T., Rieke, J., B. Sirlin, C., Song, B., Taouli, B., Yoshimitsu, K., & Koh, D. M. (2020). Consensus report from the 8th International Forum for Liver Magnetic Resonance Imaging. *European Radiology*, 30(1), 370–382. <https://doi.org/10.1007/s00330-019-06369-4>
- Zhang, H.-D., Li, X.-M., Zhang, Y.-H., Hu, F., Tan, L., Wang, F., Jing, Y., Guo, D.-J., Xu, Y., Hu, X.-L., Liu, C., & Wang, J. (2023). Evaluation of Preoperative Microvascular Invasion in Hepatocellular Carcinoma Through Multidimensional Parameter Combination Modeling Based on Gd-EOB-DTPA MRI. *Journal of Clinical and Translational Hepatology*, 11(2), 350–359. <https://doi.org/10.14218/JCTH.2021.00546>
- Zhang, L., Yu, X., Wei, W. X., Pan, X. P., Lu, L., Xia, J. J., Zheng, W., Jia, N., & Huo, L. (2020). Prediction of HCC microvascular invasion with gadobenate-enhanced MRI: correlation with pathology. *European Radiology*, 30(10), 5327–5336. <https://doi.org/10.1007/S00330-020-06895-6>